Source Attribution of Black Carbon Affecting Regional Air Quality, Premature Mortality and Glacial Deposition

Yue Qin[1], Yuanyuan Fang[2], Xiaoyuan Li[3], Vaishali Naik[4], Larry W. Horowitz[4], Junfeng Liu[5], Noah Scovronick[1], Denise L. Mauzerall[1,3,*]

[1]Woodrow Wilson School of Public Policy and International Affairs, Princeton University, Princeton, NJ 08544, USA

[2]Department of Global Ecology, Carnegie Institution for Science, Stanford University, CA 94305, USA

[3]Department of Civil and Environmental Engineering, Princeton University, Princeton, NJ 08544, USA

[4]UCAR/NOAA Geophysical Fluid Dynamics Laboratory, Princeton, Princeton, NJ 08540, USA

[5]College of Urban and Environmental Sciences, Peking University, Beijing 100080, China

[*] Correspondence to: Denise L. Mauzerall (mauzeral@princeton.edu)

Abstract

Black carbon (BC) mitigation can reduce adverse environmental impacts on climate, air quality, human health, and water resource availability. To facilitate identification of mitigation priorities, we use a state-of-the-science global coupled chemistry-climate model (AM3), with tagged regional (East Asia, South Asia, Europe and North America) and sectoral (land transport, residential, industry) anthropogenic BC emissions to identify which sources have the largest impacts on air quality, human health and glacial deposition. We find that within each tagged region, domestic emissions dominate BC surface concentrations and associated premature mortality (generally over 90%), as well as BC deposition on glaciers (~40-95% across glaciers). BC emissions occurring domestically within each tagged source region contribute roughly 1-2 orders of magnitude more to domestic BC concentrations, premature mortality, and BC deposition on regional glaciers than the same quantity of BC emitted from foreign sources. At the sectoral level, the South Asian residential sector contributes ~60% of BC associated premature mortality in South Asia and ~40-60% of total BC deposited on southern Tibetan glaciers. Our findings imply that BC mitigation within a source region, particularly from East and South Asian residential sectors, will bring the largest reductions in BC associated air pollution, premature mortality, and glacial deposition.

Keywords:

BC, Tagging method, Source-receptor matrix, Attribution efficiency, Human health.

1. Introduction

Climate change is a complex, long-term, and large-scale issue which is challenging to address in the short term due in part to the high political and economic costs of CO_2 mitigation (Keohane and Victor, 2016). However, mitigating black carbon (BC), which has a lifetime of only several days in the atmosphere and has a strong positive direct regional radiative forcing, is recognized as an effective strategy to address near-term global warming by both the scientific and diplomatic communities (CCAC, 2012; EPA, 2012; Jacobson, 2002; Kopp and Mauzerall, 2010; Ramanathan and Carmichael, 2008). Also, BC mitigation has immediate benefits for air quality, human health and water resources (via impacts on glaciers), providing strong motivation for its near-term mitigation (Bond et al., 2013; Hansen and Nazarenko, 2004; Peng et al., 2016; Shindell et al., 2012; UNEP/WMO, 2011). To help prioritize BC mitigation strategies, we quantify the regional and sectoral contributions of BC emissions on air quality, premature mortality and glacier deposition.

Epidemiological studies have linked long-term exposure to fine particulate matter in ambient air, of which BC is a key component, with an elevated risk of premature mortality (Hoek et al., 2013; Janssen, 2012; REVIHAAP, 2013). UNEP/WMO (2011)) and Shindell et al. (2012)) identified potential BC mitigation measures and estimated that by 2030 a full global implementation of these measures could avoid 2.3 million premature deaths annually due to reduced outdoor air pollution. Both studies quantified the health benefits of BC abatement under future scenarios using $PM_{2.5}$ concentration-response functions from the American Cancer Society (ACS) cohort studies (Krewski, 2009). However, the relative risk of $PM_{2.5}$ exposure found in the ACS study, which is based on ambient concentrations

63 typical of the U.S., does not accurately represent the risk associated with high levels of
64 $PM_{2.5}$ exposure in Asia, which is better represented in the Global Burden of Disease (GBD)
65 analysis (Burnett et al., 2014). Here we conduct additional analyses of source attribution
66 of regional and sectoral BC emissions to BC associated health effects, based on relative
67 risks at both high and low levels of $PM_{2.5}$ exposures, in order to prioritize mitigation efforts.
68 In addition to air quality and health considerations, BC deposition on glaciers is also of
69 immediate concern because of its effects on snow albedo, atmospheric radiative forcing,
70 and the melting rates of snow and ice that may modify the seasonality and trends of melt-
71 water supply (Kopacz et al., 2011; Ramanathan et al., 2005). Using the GEOS-Chem
72 adjoint model, Kopacz et al. (2011) identified India and China as the primary emission
73 sources of BC deposited on five glaciers in the Himalayas and Tibetan Plateau (HTP). Here
74 we further characterize the regional and sectoral anthropogenic sources depositing BC on
75 glaciers globally to prioritize BC mitigation.
76 This study goes beyond previous work and conducts an integrated assessment of the
77 source attribution of regional and sectoral present-day (2000) BC emissions on air quality,
78 premature mortality and deposition of BC on northern hemisphere glaciers. We apply a
79 source-tagging approach within a global 3-D fully coupled chemistry-climate atmospheric
80 model, Atmospheric Model version 3 (AM3). This model allows us to evaluate inter-
81 regional and inter-continental transport of BC from specific sources and regions and
82 analyze their impacts during average conditions of climate and air quality around the year
83 2000 on air quality, health and glacial deposition. This, to our knowledge, is among the
84 first trials, to conduct such an integrated assessment to evaluate the impact of BC globally.
85 The tagging technical has been applied in many literature (Brandt et al., 2012; Liu et

al., 2005, 2009a; Wang et al., 2014) and the model (AM3/GFDL) we applied also has been applied in many recent atmospheric physics/chemistry, air quality and health studies (Fang et al., 2013; Lamarque et al., 2013a; Lamarque et al., 2013b; Lee et al., 2013; Naik et al., 2013; Parrish et al., 2014; Schnell et al., 2015; Shen et al., 2017; Shindell et al., 2013; Silva et al., 2013; Stevenson et al., 2013; Voulgarakis et al., 2013; Young et al., 2013). Using AM3, a climate-chemistry coupled model, we aim to reflect the average condition of climate and air quality around the year 2000. The simulation we conduct for this study is part of an extensive assessment of the impact of BC mitigation, not only on air quality, health and glacier deposition (as shown in this paper), but also on climate (Lamarque et al., 2013b; Lee et al., 2013). As a result, it uses a present-day (2000) emission inventory developed for the Intergovernmental Panel on Climate Change Fifth Assessment Report (IPCC AR5) by Lamarque et al. (2010). The emission inventory used in our study is a standard one that the climate-chemistry community made and used in their work to simulate the 2000s climatology and chemistry (Fang et al., 2013; Lamarque et al., 2013a; Lamarque et al., 2013b; Lee et al., 2013; Naik et al., 2013; Parrish et al., 2014; Schnell et al., 2015; Shen et al., 2017; Shindell et al., 2013; Silva et al., 2013; Stevenson et al., 2013; Voulgarakis et al., 2013; Young et al., 2013). Our simulation follows the standard protocol of the Atmospheric Chemistry and Climate Model Inter-Comparison Project (ACCMIP) and uses standard emission inventories for the year 2000, so that people can inter-compare and evaluate their simulated air quality and climate impacts. In addition to running simulations for global total BC emissions from all regions and sources, we tag land anthropogenic BC emitted from four heavily-populated industrial regions (East Asia, South Asia, North America and Europe) and three sectors (land transportation, residential, and

industry) in East Asia and South Asia and identify their effects on receptors including the source regions listed above and the rest of the world (Fig. 1). Our analyses aim to identify regions and sectors where mitigation of anthropogenic BC emissions yields the greatest benefits.

2. Method

2.1 Model description

The global AM3 model is developed by the Geophysical Fluid Dynamics Laboratory (GFDL)/NOAA as the atmospheric component of their coupled general circulation model (CM3). AM3 is designed to address key emerging issues in climate science, including aerosol-cloud interactions and chemistry-climate feedbacks, and has been widerly applied in many recent studies (Fang et al., 2013; Lamarque et al., 2013a; Lamarque et al., 2013b; Lee et al., 2013; Naik et al., 2013; Parrish et al., 2014; Schnell et al., 2015; Shen et al., 2017; Shindell et al., 2013; Silva et al., 2013; Stevenson et al., 2013; Voulgarakis et al., 2013; Young et al., 2013). A finite-volume dynamical core with a cubed-sphere horizontal grid is used (2° latitude × 2.5° longitude), with horizontal resolution varying from 163 km (at the corners of each face) to 231 km (near the center of each face). Vertically, AM3 extends from the surface up to 0.01 hpa (~86 km) with 48 vertical hybrid sigma pressure levels. Vertical resolution ranges from 70 m near the earth's surface to 1 to 1.5 km near the tropopause and 3 to 4 km in much of the stratosphere (Donner et al., 2011). The model includes interactive tropospheric and stratospheric chemistry (85 species, including BC) and uses emissions (both natural and anthropogenic) to drive its chemistry and aerosol simulations.

To improve agreement between the simulated lifetime and concentrations of BC with recent observations, a BC aging scheme with updated parameters for estimating BC dry and wet deposition is implemented (Liu et al., 2011; Zhang et al., 2015a). This improved BC aging scheme considers the conversion of hydrophobic BC to hydrophilic BC, as well as the mixing of BC with other aerosols (i.e. sulfate) via characterizing the lifetime of BC with being proportional to OH radical concentrations parameterized according to observations (Liu et al., 2011; Shen et al., 2017). In terms of wet deposition, AM3 includes in-cloud and below-cloud scavenging by large-scale and convective clouds. The wet deposition flux is directly proportional to the local concentration. In-cloud scavenging of aerosols is calculated following the work of Giorgi and Chameides (1985)). In the case of convective clouds, wet deposition is only computed within the updraft plume. Below-cloud washout is only considered for large-scale precipitation and is parameterized as by Li et al. (2008)) for aerosols. Such simplified wet deposition scheme generally provides a reasonable simulation of the global mean and regional patterns of aerosol optical depth (AOD) (Donner et al., 2011) and of the spatial patterns in surface $PM_{2.5}$ (Fang et al., 2013). However, AM3 assumes that both snow and rain have the same scavenging factor and also implements "limiters" to enforce monotonicity and positive definiteness in the tracer mixing ratio profiles, which was later found to cause less effective convective removal than realistic (Paulot et al., 2016; Zhao et al., 2018). More details of parameterizations of wet deposition, particularly for aerosols, in cloud and below cloud by snow and rain are described in Fang et al. (2011)). However, AM3 assumes the same scavenging factor by snow and rain, which leads to less effective convective removal. This is because aerosols' in-cloud scavenging does not depend on the type of precipitation (rain or snow) in AM3,

thus the same collection efficiency (0.001, dimensionless) with which aerosols are collected by raindrops and snow is used. More details of parameterizations of wet deposition, particularly for aerosols, in cloud and below cloud by snow and rain are described in Fang et al. (2011)).

Earlier studies have extensively evaluated the physical (i.e., optical characteristics of aerosols) and chemical (O_3 and $PM_{2.5}$ concentrations) parameters in AM3 (Donner et al., 2011; Fang et al., 2013; Naik et al., 2013). Also, AM3 has been used in BC study and shown good comparison with other similar models (Liu et al., 2011; Shen et al., 2017; Lee et al., 2013). Liu et al. (2011) found that AM3 has better performance in simulating BC concentrations in the Arctic than all HTAP models considered by Shindell et al. (2008). They also found that AM3 would be among the best models evaluated by Koch et al. (2009). Shen et al. (2017) found that AM3 simulation results for BC in the Arctic compares well to the models in the Arctic Monitoring and Assessment Programme (AMAP), which causes an average underestimation of a factor of 2 for BC at Alert and Barrow. For this paper, we chose AM3, a chemistry-climate model because it allows us to conduct a complete and integrated assessment of the BC impacts, not only on air quality, health and glacial deposition as discussed in this paper, but also on the climate (in a parallel project). Furthermore, it allows us to evaluate inter-regional and inter-continental transport of BC and its impacts during average conditions of climate and air quality around the year 2000 (e.g., 1996-2005, a specific time slice on which the Atmospheric Chemistry and Climate Model Inter-Comparison Project -ACCMIP project focused), and thus are comparable to the ACCMIP results.

2.3 Tagging BC from various regional and sectoral sources

178 In addition to the 85 atmospheric chemical species included in the standard AM3 model,
179 we add "tagged" BC species to the model to identify the original source of BC affecting
180 air quality, premature mortality and glacier deposition. Tagged BC species undergo all the
181 dynamical, physical and chemical processes as the untagged BC, but only originate from
182 specific sources and do not affect the simulated climate. Using this method, Liu et al.
183 (2009b)) found that the differences between the sum of non-reactive tagged tracers and the
184 concentrations of the same untagged species are less than 1% at most locations thus
185 justifying the use of tagging method for source attribution analyses.

186 Thus, total BC emissions in this study include BC emissions from all anthropogenic
187 (land anthropogenic, aviation, and shipping) and natural sources. On top of that, we also
188 tag BC from land anthropogenic sources because they can be most easily mitigated and
189 collectively represent 66% of global land anthropogenic and biomass burning BC
190 emissions. To balance tracking specific emissions with computational capacity, we add
191 tagged BC tracers only from four highly-populated source regions (East Asia, South Asia,
192 Europe, and North America (see Fig.1), which contribute 18%, 7%, 6%, and 5% to global
193 land anthropogenic and biomass burning BC emissions, respectively) and sector-specific
194 tracers from the three largest emission sectors (land transportation, residential, and industry)
195 from East Asia and South Asia.

196 Our tagged BC species include BC_EA_Trans, BC_EA_Res, BC_EA_Ind,
197 BC_EA_Anthro, BC_SA_Trans, BC_SA_Res, BC_SA_Ind, BC_SA_Anthro,
198 BC_EU_Anthro, and BC_NA_Anthro. Here, 'EA', 'SA', 'EU' and 'NA', refer to BC
199 originating from East Asia, South Asia, Europe and North America, respectively. 'Trans',
200 'Res', and 'Ind' refer to land transportation, residential, and industrial sectors, respectively.

Our tagged transportation BC emissions only include BC from land transport. BC emissions from maritime transport (international shipping, domestic shipping and fishing) and aviation are included in our global total BC emissions (Lamarque et al., 2010). Residential sector includes emissions from both fossil fuel and biofuel combustion. Also, industrial sector includes emissions from both combustion (including the power sector) and non-combustion industrial processes (Lamarque et al., 2010). "Anthro" is the sum of land anthropogenic emissions from these three sectors (including both fossil fuel and biofuel combustion) and from agricultural waste burning (not including forest or grassland fires) and waste management. Implementing these tagged BC species allows us to quantify the contributions of specific anthropogenic sources (both regional and sectoral) to surface BC concentrations, the resulting premature mortality, and BC depositions on glaciers.

2.4 Estimating Premature Mortality

Some studies suggest that combustion-related particulate matter (including BC) is more toxic than other $PM_{2.5}$ components and that BC itself may act as a "universal carrier" of toxic particles (Cooke et al., 2007; Grahame and Schlesinger, 2007; Hoek et al., 2013; Morton et al., 2013; REVIHAAP, 2013). However, while efforts are growing to isolate the specific health effects of different components of fine particles ($PM_{2.5}$), evidence for differential toxicity is not fully conclusive (EPA., 2009; Janssen, 2012; REVIHAAP, 2013). Therefore, we treat BC as a fractional component of $PM_{2.5}$ to estimate BC associated premature mortality in the main analysis. Specifically, we use the $PM_{2.5}$ relative risk (RR) functions for adults (≥25 years old) from Burnett et al. (2014) for ischemic heart disease (IHD), cerebrovascular disease (stroke), chronic obstructive pulmonary disease (COPD), and lung cancer (LC), as their study covers the global range of $PM_{2.5}$ exposures, using the

equation below. Burnett et al. (2014) provides concave-shaped disease-specific integrated exposure–response (IER) functions to capture the variations in premature deaths due to changes in $PM_{2.5}$ exposures. Details for the disease-specific IHD functions can be referred to in Fig.1 in Burnett et al. (2014) and the Global Burden of Disease Study 2010 (GBD 2010) - Ambient Air Pollution Risk Model 1990 – 2010 database (http://ghdx.healthdata.org/record/global-burden-disease-study-2010-gbd-2010-ambient-air-pollution-risk-model-1990-2010).

$$\Delta Mort_i = POP_{25} * Mortbase_i * [1 - RR_i(C_{PM2.5-BC_s})/RR_i(C_{PM2.5})] \quad (1)$$

In each AM3 model grid cell, we estimate BC_s associated premature mortality from disease i ($\Delta Mort_i$) based on the adult population (POP_{25}), the baseline mortality rate in adults for disease i ($Mortbase_i$), the relative risk for disease i (RR_i) at the simulated total surface $PM_{2.5}$ concentrations ($C_{PM2.5}$), and the relative risk for disease i at the $PM_{2.5}$ concentrations without the contribution of the specific BC source ($C_{PM2.5-BC_s}$). BC_s refers to individual BC species, either the total untagged BC or each of our tagged regional or sectoral BC tracers. We obtain the 2000 global population data at 1km^2 grid level from CIESIN (2005)). Country-level age distribution and baseline mortality rates for IHD, stroke, COPD, and LC for the year 2000 are from the GBD project (http://www.healthdata.org/gbd) and are assumed uniform within each country.

In our main analysis, we assume equal toxicity between undifferentiated $PM_{2.5}$ and BC. In order to test the sensitivity of our estimated BC associated health impacts to this assumption, we also estimate health impacts using BC-specific exposure-response functions for all-cause mortality from a meta-analysis by Hoek et al. (2013). Unlike the concave integrated exposure-response functions of Burnett et al. (2014), the BC-specific

functions are (log-) linear. Therefore, for comparison, we also include a second sensitivity study using a recently-updated (log-) linear exposure-response function for all-cause mortality for undifferentiated $PM_{2.5}$ (Forestiere et al., 2014). Details of the sensitivity studies are reported in the SI.

2.5 Calculating Attribution Efficiency

To identify regions and sectors that impose the largest negative environmental impacts from each unit of BC emission, we estimate the BC attribution efficiency for air quality, premature mortality, and glacial deposition. The "attribution efficiency" for BC surface concentrations, BC associated premature mortality, or BC deposited to glaciers is defined as the magnitude of BC concentrations ($\mu g/m^3$), the number of premature deaths (cases), or the amount of BC deposition ($\mu g/m^2/day$) in receptor regions resulting from each Gg of BC emitted from a specific source region or sector ($AE_{r-s,k} = \frac{I_{r-s,k}}{E_s}$), respectively. $AE_{r-s,k}$ is the attribution efficiency for a specific type of environmental impact k (i.e., BC associated premature mortality) in receptor region r due to tagged BC tracer from source s, $I_{r-s,k}$ is the environmental impact k in receptor region r due to tagged BC tracer from source s, E_s is the emission of source s. A high attribution efficiency for a specific BC tracer indicates that a unit reduction from that source will likely result in a relatively large reduction in the negative environmental impact at the receptor region.

3. Results

3.1 Regional and Sectoral Attribution of Annual Average Simulated BC Surface Concentrations

We evaluate the effect of total global BC emissions and emissions originating from each of our tagged regions and sectors on simulated annual average surface BC concentrations. Simulated global annual average BC surface concentrations exhibit hotspots in Asia, particularly in eastern China and the Indo-Gangetic plain of India (Fig. 2), with the highest concentrations found in Shandong province in China (~3.5 μg/m^3). BC surface concentrations in Europe and the United States are much lower - roughly 0.05-1 μg/m^3 and 0.05-0.5 μg/m^3, respectively. BC emissions from each of our four tagged regions are primarily concentrated within their respective source regions (Fig. 2).

We also present the simulated annual average population-weighted (P-W) BC surface concentrations ($C_{PW}(R) = \frac{\sum_{i=1}^{n} Pop_i\,(R) * C_i(R)}{\sum_{i=1}^{n} Pop_i(R)}$) in the four tagged regions in Fig. 3. $C_{PW}(R)$ refers to P-W annual average BC surface concentrations in each tagged region R, Pop_i refers to population in grid i, and $C_i(R)$ refers to model simulated BC concentrations in grid i in region R. As shown in Fig. 3, East Asia (1.7 μg/m^3) and South Asia (1.1 μg/m^3), the two regions with the largest population, also have the highest P-W concentrations, followed by Europe (0.5 μg/m^3) and North America (0.4 μg/m^3). We find that domestic anthropogenic BC emissions dominate that region's P-W BC surface concentrations, accounting for 96%, 93%, 89% and 93% of surface BC concentrations over East Asia, South Asia, Europe and North America, respectively. Any individual foreign contributions to P-W BC concentrations are generally below 1%. Within each region, the sectors that contribute most to domestic P-W BC concentrations are the industrial sector in East Asia (~50%) and the residential sector in South Asia (~60%). We find that in East Asia and South Asia, sectoral contributions to P-W BC surface concentrations are roughly proportional to their domestic emission shares.

3.2 Regional and Sectoral Attribution of BC Associated Premature Mortality

We estimate global total BC associated premature mortality to be 106,000 annually (95% confidence interval, CI, 45,000-143,000, see Table 1 and Supplementary Fig. S1), with ranges reflecting the low and high estimates of relative risks for $PM_{2.5}$ exposure reported in Burnett et al. (2014). As shown in Fig. 4 and Fig. S2, high BC associated premature mortality primarily occurs in East Asia (over 10 BC associated premature deaths/1000 km^2 in eastern China) and South Asia (1-10 BC associated premature deaths/1000 km^2 across India), both regions with high BC concentrations and dense population. Accordingly, approximately half of the global total BC associated premature deaths occur in East Asia, followed by 17% in South Asia. In contrast, BC associated premature mortality is relatively low in Europe (0.1-10 premature deaths/ 1000 km^2) and North America (0.1-1 premature deaths/ 1000 km^2 in eastern U.S.), contributing approximately 12% and 4% of the global total BC associated premature deaths, respectively.

We further quantify the source attribution of regional and sectoral BC emissions on BC associated premature mortality (Table 1). In each region, emissions from that region (domestic emissions) generally account for over 90% of total BC associated premature mortality while the contribution from any given foreign region is typically below 1%. From the sectoral perspective, domestic BC emissions from the industrial (~50%) and residential (~35%) sectors make up ~85% of BC associated premature deaths occurring in East Asia. The residential sector dominates (~60%) BC associated premature deaths in South Asia. Similar to BC surface concentrations, in both East Asia and South Asia, sectoral contributions to BC associated premature mortality are roughly proportional to their respective emission shares.

Our sensitivity analyses (Fig. S1) demonstrate that the health impacts from BC exposure would be much higher if BC toxicity is greater than that of typical $PM_{2.5}$. We find that using BC-specific relative risks leads to a mortality burden that is 14 times higher than what we obtain with the cause-specific, concave functions for $PM_{2.5}$ reported in Burnett et al. (2014). Only a relatively small part of the difference is attributable to assumptions about the shape of the exposure-response relationship (log-linear versus concave) and the number of causes (all causes versus four causes) (Fig. S1). The primary difference results from the difference in toxicity of the $PM_{2.5}$ components. This indicates that our main estimates of the mortality burden associated with BC exposure, which are based on changes to total $PM_{2.5}$ concentrations, are conservative should evidence of enhanced toxicity of BC be confirmed.

3.3 Regional and Sectoral Attribution of BC Deposition on Northern Hemispheric Glaciers

We analyze BC deposition at the specific locations of individual glaciers in each region. Detailed geographic information of glaciers evaluated are shown in Fig. S3 and Table S1. Due to notable spatial heterogeneities and seasonal variations for BC deposition, we quantify the seasonal contributions of regional and sectoral anthropogenic BC emissions to BC deposition on glaciers in Asia, Europe, North America and the Arctic, respectively (Fig. S4).

3.3.1 Asia Glaciers

In Asia, we focus on the Himalayan Tibetan Plateau (HTP) glaciers. For nearly all these glaciers, seasonal contributions of land anthropogenic BC from South Asia and East Asia represent between ~40%-95% of total BC deposition. Southern Tibetan glaciers receive a relatively large total BC deposition (Fig. 5a). On these glaciers, South Asian land anthropogenic BC emissions alone account for ~60-90% of total BC deposition across seasons, of which ~40-60% is attributed to the residential sector. This is consistent with earlier findings that South Asia is the major source of BC in southern HTP (Zhang et al., 2015b). Besides, due to the Asian monsoon that carries emissions from South Asia northwards, these glaciers usually have the largest total deposition in summer, when South Asian emissions account for 80-90% of total BC deposition (Fig. 5a). In contrast, the largest East Asian contribution to BC deposition on these glaciers occurs in October (i.e., ~ 30% in Zuoqiupu), in part because of the returning winter monsoonal flow. In other seasons, East Asia contributes less than 10% of total BC deposition. Regional contributions to BC deposition on central and southern HTP glaciers are similar, though total deposition

on central HTP glaciers is much lower than on southern HTP glaciers (Fig. 5a). In the northern Tibetan Plateau, we generally find a dominant East Asian contribution in summer among our tagged tracers, which has also been identified in previous studies (Li et al., 2016; Zhang et al., 2015b). However, our study finds that south Asian land anthropogenic BC emissions mostly dominate BC deposition in the northern Tibetan Plateau in other seasons, though East Asian emissions are also important (Fig. 5b). Additionally, European land anthropogenic BC emissions deposit 1-10% of total BC on northern Tibetan glaciers, particularly on Haxilegen River and Mt. Muztagh glaciers, with the largest contributions in summer. Kopacz et al. (2011) identify a strong snow-albedo driven seasonal cycle (lowest in winter and highest in summer) in radiative forcing on northern Tibetan glaciers, indicating an enhancement of potential glacial melting due to glacial deposition of BC in summer. Thus, East Asian land anthropogenic BC emissions, which contribute most to northern HTP glacial deposition in summer, are likely to enhance northern HTP glacial melting most.

3.3.2 European and North American Glaciers

As shown in Fig. 5c, anthropogenic BC emissions within each source region dominate BC deposition over both European and North American glaciers in all seasons. For European glaciers, domestic land anthropogenic BC emissions contribute ~50-90% of total BC deposition, depending on the season. In comparison, contributions from East Asia, South Asia and North America are each generally below 5%, with the remaining originating from either wildfires or BC emission sources outside the tagged regions.

Similarly, North American land anthropogenic BC emissions contribute ~40-80% of BC deposition on North American glaciers. Notably, East Asian land anthropogenic BC emissions contribute ~20% to BC deposition on western US glaciers (i.e., Washington state and the Sierra Nevada mountains) during non-summer seasons, with roughly 9% and 7% attributable to the East Asian industrial and residential sectors, respectively.

3.3.3 Arctic Glaciers

BC deposition on Arctic glaciers is of particular concern due to their critical role in affecting the climate via positive feedbacks on melting sea ice (McConnell et al., 2007; Ramanathan and Carmichael, 2008). We find that European (~25%), East Asian (~13%), North American (~7%), and South Asian (~3%) land anthropogenic emissions together contribute about half of annual average total BC deposition to the Arctic (> 67° N), though large variations exist depending on the geographic location of glaciers and the season (Fig. 5d and Fig. S4). The other half of BC deposition over the Arctic may come from emissions from biomass burning (wildfires) and other untagged sources. For example, BC from biomass burning has been found to make up 40% of BC in Arctic air (Winiger et al., 2016),

385 and to account for over 90% of BC in Arctic snow when counted along with biofuel (Hegg
386 et al., 2009).

387 Fig. 5d shows the seasonal contributions of our tagged anthropogenic BC emissions to
388 BC deposition on Arctic glaciers in Alaska, Greenland, and Russia. Our tagged
389 anthropogenic BC emissions from four tagged regions together explain roughly 60-80% of
390 the total BC deposition on Alaskan and Greenland glaciers and about 40%-60% on Russian
391 glaciers in non-summer seasons. The lower contribution of tagged emissions on Russian
392 glaciers suggests that untagged Russian emissions (particularly domestic biomass burning
393 may contribute roughly half of total Russian BC emissions) are an important source of BC
394 deposition (Lamarque et al., 2010). Contributions from untagged wildfire emissions are
395 particularly notable in summer, when our tagged anthropogenic BC emissions together
396 only explain ~20%, ~45%, and ~25% of total BC deposition over Alaska, Greenland, and
397 Russian glaciers. This is most likely due to large contributions to Arctic BC from European
398 and Siberian boreal fires in summer (Bond et al., 2013; Hegg et al., 2009; McConnell et
399 al., 2007).

400 In our simulations, Alaskan glaciers, depending on the season, receive ~10-35% of their
401 total BC deposition from East Asian land anthropogenic BC emissions, significantly more
402 than from Europe (~3-20%), North America (~2-10%) or South Asia (~1-5%). For
403 southern Greenland glaciers (i.e., Dye2), North American land anthropogenic BC
404 emissions, depending on the season, contribute ~20-30% of BC deposition, followed by
405 Europe with ~10-20%. In comparison, among our tagged emissions, European land
406 anthropogenic BC emissions dominate BC deposition onto northern Greenland glaciers
407 (~20-50% depending on the season). We also find that of our tagged emissions, European

and East Asian land anthropogenic BC emissions dominate BC deposition over western and eastern Russian glaciers, respectively.

3.4 Attribution Efficiency of BC Impacts on Air Quality, Premature Mortality, and Deposition on Glaciers

We estimate the attribution efficiency for annual average P-W BC concentrations, BC associated premature mortality, and BC deposition on glaciers (Supplementary Tables S2-S4).

As shown in Supplementary Table S2, across regions, each unit of BC emission in South Asia contributes the most (ie. has the largest attribution efficiency) to BC surface concentrations within its own source region (approximately 60%, 80%, and 95% higher than attribution efficiency in East Asia, Europe, and North America, respectively). This is primarily because the annual average lifetime of BC from South Asia is longer than from other regions mainly due to less efficient wet deposition (Shindell et al., 2008). In comparison, East Asia has the largest attribution efficiency in BC-associated premature deaths within its own source region, roughly 35 (11-47) premature deaths per Gg BC. In comparison, South Asia, Europe, and North America have attribution efficiencies of 28 (13-45), 25 (15-31) and 12 (7-12) premature deaths per Gg BC of their own emissions, respectively (Supplementary Table S3). Ranges of premature mortality attribution efficiency are due to uncertainties in the $PM_{2.5}$ relative risks. Higher attribution efficiency for BC associated premature mortality in East Asia primarily occurs because the adult population in East Asia was ~1.5, ~2.2, and ~4.2 times higher than in South Asia, Europe, and North America in the year 2000, respectively. Nevertheless, the number of adults in India has grown rapidly since 2000

(http://esa.un.org/unpd/wpp/Download/Standard/Population/), and is estimated to surpass China around 2040 (Fig. S5). Thus, the attribution efficiency for BC associated premature mortality will likely increase in South Asia.

We find that South Asian emissions have the largest BC deposition attribution efficiency over Asian glaciers (Table S4). Specifically, in southern and central (northern) Tibetan glaciers, each unit of South Asian emissions results in 10-100 times (1-4 times) more BC deposition than the same quantity of East Asian emissions. Similarly, for European and North American glaciers, domestic BC emissions have 1-2 orders of magnitude larger attribution efficiencies for BC deposition than BC emissions from any foreign region. Notably, for most Arctic glaciers, anthropogenic BC emissions from Europe generally have the largest BC deposition attribution efficiency among our tagged tracers. However, the largest attribution efficiency for southern Greenland glaciers is from North America.

Sectoral differences affecting the attribution efficiency of BC concentrations, premature mortality, and deposition on glaciers are generally small. However, our estimated premature mortality attributed to emissions from the residential sector does not account for indoor air pollution, which resulted in over 3 million premature deaths worldwide in 2000 (http://www.healthdata.org/gbd). Thus, including the effects of indoor air pollution would substantially increase the attribution efficiency of total (indoor plus outdoor) BC associated premature mortality associated with the residential sector.

4. Discussion

453 To evaluate the potential benefits of various BC mitigation strategies, this study
454 systematically quantifies the source attribution of regional and sectoral BC emissions on
455 air quality, premature mortality and deposition on glaciers by tagging land anthropogenic
456 BC tracers from four regions and three sectors within a global coupled chemistry-climate
457 model.

458 We find that intra-regional emissions usually contribute over 90% of BC surface
459 concentrations and associated premature mortality, as well as ~40-95% of BC deposition
460 on glaciers within each region. Additionally, domestic BC emissions generally contribute
461 approximately 1-2 orders of magnitude more to BC concentrations, associated premature
462 deaths, and BC deposition on glaciers than the same quantity of foreign emissions. This
463 indicates that reducing domestic BC emissions can bring both the largest total reduction
464 potential and the highest reduction efficiency for the BC associated environmental impacts
465 we evaluate in this work.

466 Across regions, people in East Asia and South Asia are exposed to the highest BC
467 surface concentrations and suffer from the largest resulting premature mortality. Among
468 the 106,000 (95% CI: 45,000-143,000) cases of BC associated premature deaths globally,
469 ~70% occur in Asia. Within either East Asia or South Asia, sectoral contributions to BC
470 surface concentrations and associated premature mortality, and to BC deposition on
471 glaciers are roughly proportional to their emission shares. For instance, the South Asian
472 residential sector, which accounts for approximately 60% of total regional land
473 anthropogenic BC emissions, contributes ~60% of domestic population-weighted (P-W)
474 BC concentrations and associated premature mortality, as well as ~40-60% of total BC
475 deposition on southern Tibetan glaciers.

476 Regarding attribution efficiency, the largest attribution efficiency for health impacts
477 occurs in East Asia, where it is approximately 20%, 40%, and 200% larger than in South
478 Asia, Europe, and North America, respectively, primarily due to the co-location of dense
479 population and high BC emissions in East Asia. Importantly, the health impacts from each
480 unit of BC emission have increased significantly in South Asia over the past decade due to
481 rapid population growth. Sectoral differences in attribution efficiency for BC associated
482 premature mortality from outdoor air pollution are usually small. However, BC emission
483 from the residential sector may be particularly important given the adverse impacts of
484 indoor air pollution and associated health burden (Smith and Mehta, 2003). Overall, this
485 implies that BC mitigation may be particularly beneficial in Asia, especially from the
486 residential sector.
487 Although domestic BC dominates regional impacts, foreign contributions to premature
488 mortality and BC deposition on glaciers do occur, particularly for regions with little
489 domestic BC emission sources. For instance, East Asian anthropogenic BC emissions are
490 a large contributor to BC deposition over the Arctic, especially on Alaskan glaciers (~10-
491 35% across seasons). Thus, even though the Arctic countries can work together through
492 the Arctic Council to mitigate emissions of their own short-lived climate forcers (Sand et
493 al., 2016), our study suggests it would be beneficial for them to facilitate East Asian BC
494 emission reductions, particularly for Alaskan glaciers. Over the past decade, international
495 efforts to facilitate BC mitigation in developing countries by institutions such as the
496 Climate and Clean Air Coalition (CCAC, 2012) and Global Alliance for Clean Cookstoves
497 (GACC, 2010) have made some progress at reducing emissions. Continuing international
498 collaboration for existing projects as well as local capacity building, particularly in South

499 Asia and East Asia, will be beneficial to ensure sustainable and cost-effective BC
500 mitigation in these regions, especially in the residential sector (Baron et al., 2015; UNEP,
501 2011).

502 We recognize that results in this study are subject to various uncertainties from emission
503 inventories, the representation of BC in our model, and the relative toxicity of BC in
504 comparison to other $PM_{2.5}$ components. BC emission inventory studies report large
505 uncertainties (i.e., a factor of 2-4 in Asia) due to challenges in quantifying particle
506 emissions from incomplete combustion and in determining BC emitting activity levels
507 (Bond et al., 2013; Cohen and Wang, 2014; Qin and Xie, 2011a, b, 2012; Zhao et al., 2011).
508 Also, although this version of the AM3 model uses an updated representation of BC aging
509 (Liu et al., 2011; Zhang et al., 2015a), it still does not perfectly capture the chemical-
510 physical transformation of BC. Thus, better quantification of the BC emission inventory
511 and model development advances will be valuable in improving BC source attribution
512 estimates. In addition, our study identifies substantial uncertainties (roughly a factor of 15)
513 in BC associated health impacts primarily due to differences in estimates of the toxicity of
514 BC compared with $PM_{2.5}$. Thus increasing efforts to differentiate the toxicity of various
515 $PM_{2.5}$ components are needed to better identify the health impacts of BC. As our simulated
516 BC concentrations from the global coarse-resolution chemistry-cliamte model tend to
517 underestimate BC concentrations especially in urban areas, and we assume the same
518 toxicity for BC with other $PM_{2.5}$ components, our estimated BC associated premature
519 deaths are conservative. However, we believe that such underestimates are unlikely to
520 change our qualitative conclusions in terms of the dominant local benefits of BC
521 mitigation.

Our study focuses on year 2000 to be comparable to ACCMIP results. However, BC emissions have evolved over the past two decades (Bond et al., 2013; Mao et al., 2016; Qin and Xie, 2012). Granier et al. (2011) have made a comprehensive comparison of various bottom-up anthropogenic and biomass burning emission inventories between 1980-2010. Their comparison indicates that globally, all emission inventories agree that anthropogenic BC emissions increased from 2000-2010 although the rate of increase decreased around 2005. Granier et al. (2011) also found that all emission inventories suggested a strong increase in anthropogenic BC emissions from China and India during this period, though different emission inventories identified either small increases or decreases in anthropogenic BC emissions in Western and Central Europe as well as in the United States. The increasing trend in China and India is consistent with a few later Asian-focused studies. For example, Bond et al. (2013) found that Asian BC emissions increased from ~7.5 Tg/yr in 2000 to 9.8 Tg/yr in 2005. Likewise, Qin and Xie (2012) found that BC emissions in China, the world's largest BC emitter, increased from ~1.2 Tg/yr in 2000 to ~1.9 Tg/yr in 2009. Similar global and regional trends are also captured in the Representative Concentration Pathways (RCP) scenarios. The RCP8.5 has been especially considered to be a reasonable extension of the ACCMIP simulations beyond 2000 (Granier et al., 2011)). All RCP scenarios also show increases in BC emissions from 2000 to 2010, though they also suggest that total BC emissions peaked in 2010 and will reach a similar emission level to 2000 in 2020 (Fig. S6a). Nevertheless, at the regional level, BC emissions show a consistent increasing trend in Asia from 2000 to 2020, though it has been decreasing in the OECD countries (including Europe and North America) during the same period (Fig. S6b). Meanwhile, global population has increased from ~6 billion in 2000 to ~7 billion in 2015,

545 with particularly large growth in South and East Asia. These region-specific trends in both
546 BC emissions and population growth suggest that the source attribution of south and east
547 Asian BC emissions on air quality, health and glacier deposition is likely to be even more
548 important in more recent years than what we identified in this study.
549
550 **Acknowledgement**
551 Y. Qin and Y. Fang thank Princeton University's Woodrow Wilson School of Public and
552 International Affairs for graduate and post-doctoral funding.
553
554 **Supplementary information** accompanies this paper.
555 **Competing Interests:** The authors declare that they have no competing interests.
556
557

References

Baron RE, Montgomery WD, Tuladhar SD. An Analysis of Black Carbon Mitigation as A Response to Climate Change. Copenhagen consensus on climate, 2015.

Bond TC, Doherty SJ, Fahey DW, Forster PM, Berntsen T, DeAngelo BJ, et al. Bounding the role of black carbon in the climate system: A scientific assessment. Journal of Geophysical Research-Atmospheres 2013; 118: 5380-5552.

Brandt J, Silver JD, Frohn LM, Geels C, Gross A, Hansen AB, et al. An integrated model study for Europe and North America using the Danish Eulerian Hemispheric Model with focus on intercontinental transport of air pollution. Atmospheric Environment 2012; 53: 156-176.

Burnett RT, Pope CA, Ezzati M, Olives C, Lim SS, Mehta S, et al. An Integrated Risk Function for Estimating the Global Burden of Disease Attributable to Ambient Fine Particulate Matter Exposure. Environmental Health Perspectives 2014; 122: 397-403.

CCAC. The Climate and Clean Air Coalition to Reduce Short-Lived Climate Pollutants. http://www.ccacoalition.org/en. 2012.

CIESIN. Center for International Earth Science Information Network, Columbia University; and Centro Internacional de Agricultura Tropical (CIAT), Gridded Population of the World, Version 3 (GPWv3). Palisades, NY: Socioeconomic Data and Applications Center (SEDAC), Columbia University, available at: http://sedac.ciesin.columbia.edu/gpw. 2005.

Cohen JB, Wang C. Estimating global black carbon emissions using a top-down Kalman Filter approach. Journal of Geophysical Research-Atmospheres 2014; 119: 307-323.

Cooke RM, Wilson AM, Tuomisto JT, Morales O, Tainio M, Evans JS. A Probabilistic characterization of the relationship between fine particulate matter and mortality: Elicitation of European experts. Environmental Science & Technology 2007; 41: 6598-6605.

584 Donner LJ, Wyman BL, Hemler RS, Horowitz LW, Ming Y, Zhao M, et al. The Dynamical Core,
585 Physical Parameterizations, and Basic Simulation Characteristics of the Atmospheric
586 Component AM3 of the GFDL Global Coupled Model CM3. Journal of Climate 2011;
587 24: 3484-3519.
588 EPA. Report to Congress on Black Carbon.
589 https://www3.epa.gov/blackcarbon/2012report/Chapter4.pdf. 2012.
590 EPA. 2009 Final Report: Integrated Science Assessment for Particulate Matter. U.S.
591 Environmental Protection Agency, Washington, DC, EPA/600/R-08/139F, 2009. (U.S.
592 EPA). 2009.
593 Fang Y, Naik V, Horowitz LW, Mauzerall DL. Air pollution and associated human mortality: the
594 role of air pollutant emissions, climate change and methane concentration increases from
595 the preindustrial period to present. Atmospheric Chemistry and Physics 2013; 13: 1377-
596 1394.
597 Fang YY, Fiore AM, Horowitz LW, Gnanadesikan A, Held I, Chen G, et al. The impacts of
598 changing transport and precipitation on pollutant distributions in a future climate. Journal
599 of Geophysical Research-Atmospheres 2011; 116.
600 Forestiere F, Kan H, Cohen A. Updated exposure-response functions available for estimating
601 mortality impacts. 2014.
602 GACC. Global Alliance for Clean Cookstoves. http://cleancookstoves.org. 2010.
603 Giorgi F, Chameides WL. The Rainout Parameterization in a Photochemical Model. Journal of
604 Geophysical Research-Atmospheres 1985; 90: 7872-7880.
605 Grahame TJ, Schlesinger RB. Health effects of airborne particulate matter: Do we know enough
606 to consider regulating specific particle types or sources? Inhalation Toxicology 2007; 19:
607 457-481.

608 Granier C, Bessagnet B, Bond T, D'Angiola A, van der Gon HD, Frost GJ, et al. Evolution of
609 anthropogenic and biomass burning emissions of air pollutants at global and regional
610 scales during the 1980-2010 period. Climatic Change 2011; 109: 163-190.
611 Hansen J, Nazarenko L. Soot climate forcing via snow and ice albedos. Proceedings of the
612 National Academy of Sciences of the United States of America 2004; 101: 423-428.
613 Hegg DA, Warren SG, Grenfell TC, Doherty SJ, Larson TV, Clarke AD. Source Attribution of
614 Black Carbon in Arctic Snow. Environmental Science & Technology 2009; 43: 4016-
615 4021.
616 Hoek G, Krishnan RM, Beelen R, Peters A, Ostro B, Brunekreef B, et al. Long-term air pollution
617 exposure and cardio-respiratory mortality: a review. Environmental Health 2013; 12.
618 Jacobson MZ. Control of fossil-fuel particulate black carbon and organic matter, possibly the
619 most effective method of slowing global warming. Journal of Geophysical Research-
620 Atmospheres 2002; 107.
621 Janssen NA, Gerlofs-Nijland, M.E., Lanki, T., Salonen, R.O., Cassee, F., Hoek, G., Fischer, P.,
622 Brunekreef, B., Krzyzanowski, M. Health effects of black carbon. World Health
623 Organization Regional Office For Europe, 2012.
624 Keohane RO, Victor DG. Cooperation and discord in global climate policy. Nature Climate
625 Change 2016; 6: 570-575.
626 Koch D, Schulz M, Kinne S, McNaughton C, Spackman JR, Balkanski Y, et al. Evaluation of
627 black carbon estimations in global aerosol models. Atmospheric Chemistry and Physics
628 2009; 9: 9001-9026.
629 Kopacz M, Mauzerall DL, Wang J, Leibensperger EM, Henze DK, Singh K. Origin and radiative
630 forcing of black carbon transported to the Himalayas and Tibetan Plateau. Atmospheric
631 Chemistry and Physics 2011; 11: 2837-2852.

632 Kopp RE, Mauzerall DL. Assessing the climatic benefits of black carbon mitigation. Proceedings
633 of the National Academy of Sciences of the United States of America 2010; 107: 11703-
634 11708.
635 Krewski D, Jerrett, M., Burnett, R. T., Ma, R., Hughes, E., Shi, Y., Turner, M. C., Pope III, C. A.,
636 Thurston, G., Calle, E. E., and Thun, M. J. Extended Follow-Up and Spatial Analysis of
637 the American Cancer Society Study Linking Particulate Air Pollution and Mortailty. HEI
638 Research Report. Health Effects Institute, Boston, MA. 2009.
639 Lamarque JF, Bond TC, Eyring V, Granier C, Heil A, Klimont Z, et al. Historical (1850-2000)
640 gridded anthropogenic and biomass burning emissions of reactive gases and aerosols:
641 methodology and application. Atmospheric Chemistry and Physics 2010; 10: 7017-7039.
642 Lamarque JF, Dentener F, McConnell J, Ro CU, Shaw M, Vet R, et al. Multi-model mean
643 nitrogen and sulfur deposition from the Atmospheric Chemistry and Climate Model
644 Intercomparison Project (ACCMIP): evaluation of historical and projected future
645 changes. Atmospheric Chemistry and Physics 2013a; 13: 7997-8018.
646 Lamarque JF, Shindell DT, Josse B, Young PJ, Cionni I, Eyring V, et al. The Atmospheric
647 Chemistry and Climate Model Intercomparison Project (ACCMIP): overview and
648 description of models, simulations and climate diagnostics. Geoscientific Model
649 Development 2013b; 6: 179-206.
650 Lee YH, Lamarque JF, Flanner MG, Jiao C, Shindell DT, Berntsen T, et al. Evaluation of
651 preindustrial to present-day black carbon and its albedo forcing from Atmospheric
652 Chemistry and Climate Model Intercomparison Project (ACCMIP). Atmospheric
653 Chemistry and Physics 2013; 13: 2607-2634.
654 Li CL, Bosch C, Kang SC, Andersson A, Chen PF, Zhang QG, et al. Sources of black carbon to
655 the Himalayan-Tibetan Plateau glaciers. Nature Communications 2016; 7.

656 Li F, Ginoux P, Ramaswamy V. Distribution, transport, and deposition of mineral dust in the
657 Southern Ocean and Antarctica: Contribution of major sources. Journal of Geophysical
658 Research-Atmospheres 2008; 113.
659 Liu JF, Fan SM, Horowitz LW, Levy H. Evaluation of factors controlling long-range transport of
660 black carbon to the Arctic. Journal of Geophysical Research-Atmospheres 2011; 116.
661 Liu JF, Mauzerall DL, Horowitz LW. Analysis of seasonal and interannual variability in
662 transpacific transport. Journal of Geophysical Research-Atmospheres 2005; 110.
663 Liu JF, Mauzerall DL, Horowitz LW. Evaluating inter-continental transport of fine aerosols:(2)
664 Global health impact. Atmospheric Environment 2009a; 43: 4339-4347.
665 Liu JF, Mauzerall DL, Horowitz LW, Ginoux P, Fiore AM. Evaluating inter-continental transport
666 of fine aerosols: (1) Methodology, global aerosol distribution and optical depth.
667 Atmospheric Environment 2009b; 43: 4327-4338.
668 Mao YH, Liao H, Han YM, Cao JJ. Impacts of meteorological parameters and emissions on
669 decadal and interannual variations of black carbon in China for 1980-2010. Journal of
670 Geophysical Research-Atmospheres 2016; 121: 1822-1843.
671 McConnell JR, Edwards R, Kok GL, Flanner MG, Zender CS, Saltzman ES, et al. 20th-century
672 industrial black carbon emissions altered arctic climate forcing. Science 2007; 317: 1381-
673 1384.
674 Morton L, Chen L, Gordon T, Ito K, Thurston GD. HEALTH EFFECTS INSTITUTE (HEI).
675 National Particle Component Toxicity (NPACT) Initiative: Integrated Epidemiologic and
676 Toxicologic Studies of the Health Effects of Particulate Matter Components. 2013.
677 Naik V, Voulgarakis A, Fiore AM, Horowitz LW, Lamarque JF, Lin M, et al. Preindustrial to
678 present-day changes in tropospheric hydroxyl radical and methane lifetime from the
679 Atmospheric Chemistry and Climate Model Intercomparison Project (ACCMIP).
680 Atmospheric Chemistry and Physics 2013; 13: 5277-5298.

Parrish DD, Lamarque JF, Naik V, Horowitz L, Shindell DT, Staehelin J, et al. Long-term changes in lower tropospheric baseline ozone concentrations: Comparing chemistry-climate models and observations at northern midlatitudes. Journal of Geophysical Research-Atmospheres 2014; 119: 5719-5736.

Paulot F, Ginoux P, Cooke WF, Donner LJ, Fan S, Lin MY, et al. Sensitivity of nitrate aerosols to ammonia emissions and to nitrate chemistry: implications for present and future nitrate optical depth. Atmospheric Chemistry and Physics 2016; 16: 1459-1477.

Peng JF, Hu M, Guo S, Du ZF, Zheng J, Shang DJ, et al. Markedly enhanced absorption and direct radiative forcing of black carbon under polluted urban environments. Proceedings of the National Academy of Sciences of the United States of America 2016; 113: 4266-4271.

Qin Y, Xie SD. Estimation of county-level black carbon emissions and its spatial distribution in China in 2000. Atmospheric Environment 2011a; 45: 6995-7004.

Qin Y, Xie SD. Historical estimation of carbonaceous aerosol emissions from biomass open burning in China for the period 1990-2005. Environmental Pollution 2011b; 159: 3316-3323.

Qin Y, Xie SD. Spatial and temporal variation of anthropogenic black carbon emissions in China for the period 1980-2009. Atmospheric Chemistry and Physics 2012; 12: 4825-4841.

Ramanathan V, Carmichael G. Global and regional climate changes due to black carbon. Nature Geoscience 2008; 1: 221-227.

Ramanathan V, Chung C, Kim D, Bettge T, Buja L, Kiehl JT, et al. Atmospheric brown clouds: Impacts on South Asian climate and hydrological cycle. Proceedings of the National Academy of Sciences of the United States of America 2005; 102: 5326-5333.

REVIHAAP. Review of evidence on health aspects of air pollution – REVIHAAP Project. Technical Report. World Health Organization. 2013.

706 Sand M, Berntsen TK, von Salzen K, Flanner MG, Langner J, Victor DG. Response of Arctic
707 temperature to changes in emissions of short-lived climate forcers. Nature Climate
708 Change 2016; 6: 286-+.
709 Schnell JL, Prather MJ, Josse B, Naik V, Horowitz LW, Cameron-Smith P, et al. Use of North
710 American and European air quality networks to evaluate global chemistry-climate
711 modeling of surface ozone. Atmospheric Chemistry and Physics 2015; 15: 10581-10596.
712 Shen ZY, Ming Y, Horowitz LW, Ramaswamy V, Lin MY. On the Seasonality of Arctic Black
713 Carbon. Journal of Climate 2017; 30: 4429-4441.
714 Shindell D, Kuylenstierna JCI, Vignati E, van Dingenen R, Amann M, Klimont Z, et al.
715 Simultaneously Mitigating Near-Term Climate Change and Improving Human Health
716 and Food Security. Science 2012; 335: 183-189.
717 Shindell DT, Chin M, Dentener F, Doherty RM, Faluvegi G, Fiore AM, et al. A multi-model
718 assessment of pollution transport to the Arctic. Atmospheric Chemistry and Physics
719 2008; 8: 5353-5372.
720 Shindell DT, Lamarque JF, Schulz M, Flanner M, Jiao C, Chin M, et al. Radiative forcing in the
721 ACCMIP historical and future climate simulations. Atmospheric Chemistry and Physics
722 2013; 13: 2939-2974.
723 Silva RA, West JJ, Zhang YQ, Anenberg SC, Lamarque JF, Shindell DT, et al. Global premature
724 mortality due to anthropogenic outdoor air pollution and the contribution of past climate
725 change. Environmental Research Letters 2013; 8.
726 Smith KR, Mehta S. The burden of disease from indoor air pollution in developing countries:
727 comparison of estimates. International Journal of Hygiene and Environmental Health
728 2003; 206: 279-289.
729 Stevenson DS, Young PJ, Naik V, Lamarque JF, Shindell DT, Voulgarakis A, et al. Tropospheric
730 ozone changes, radiative forcing and attribution to emissions in the Atmospheric

731 Chemistry and Climate Model Intercomparison Project (ACCMIP). Atmospheric
732 Chemistry and Physics 2013; 13: 3063-3085.
733 UNEP. Near-term Climate Protection and Clean Air Benefits: Actions for Controlling Short-
734 Lived Climate Forcers. United Nations Environment Programme (UNEP). 2011.
735 UNEP/WMO. Integrated Assessment of Black Carbon and Tropospheric Ozone. United Nations
736 Environment Programme (UNEP). 2011.
737 Voulgarakis A, Naik V, Lamarque JF, Shindell DT, Young PJ, Prather MJ, et al. Analysis of
738 present day and future OH and methane lifetime in the ACCMIP simulations.
739 Atmospheric Chemistry and Physics 2013; 13: 2563-2587.
740 Wang HL, Rasch PJ, Easter RC, Singh B, Zhang RD, Ma PL, et al. Using an explicit emission
741 tagging method in global modeling of source-receptor relationships for black carbon in
742 the Arctic: Variations, sources, and transport pathways. Journal of Geophysical Research-
743 Atmospheres 2014; 119: 12888-12909.
744 Winiger P, Andersson A, Eckhardt S, Stohl A, Gustafsson O. The sources of atmospheric black
745 carbon at a European gateway to the Arctic. Nature Communications 2016; 7.
746 Young PJ, Archibald AT, Bowman KW, Lamarque JF, Naik V, Stevenson DS, et al. Pre-
747 industrial to end 21st century projections of tropospheric ozone from the Atmospheric
748 Chemistry and Climate Model Intercomparison Project (ACCMIP). Atmospheric
749 Chemistry and Physics 2013; 13: 2063-2090.
750 Zhang J, Liu J, Tao S, Ban-Weiss GA. Long-range transport of black carbon to the Pacific Ocean
751 and its dependence on aging timescale. Atmospheric Chemistry and Physics 2015a; 15:
752 11521-11535.
753 Zhang R, Wang H, Qian Y, Rasch PJ, Easter RC, Ma PL, et al. Quantifying sources, transport,
754 deposition, and radiative forcing of black carbon over the Himalayas and Tibetan Plateau.
755 Atmospheric Chemistry and Physics 2015b; 15: 6205-6223.

Zhao M, Golaz JC, Held IM, Guo H, Balaji V, Benson R, et al. The GFDL Global Atmosphere and Land Model AM4.0/LM4.0:2. Model Description, Sensitivity Studies, and Tuning Strategies. Journal of Advances in Modeling Earth Systems 2018; 10: 735-769.

Zhao Y, Nielsen CP, Lei Y, McElroy MB, Hao J. Quantifying the uncertainties of a bottom-up emission inventory of anthropogenic atmospheric pollutants in China. Atmospheric Chemistry and Physics 2011; 11: 2295-2308.

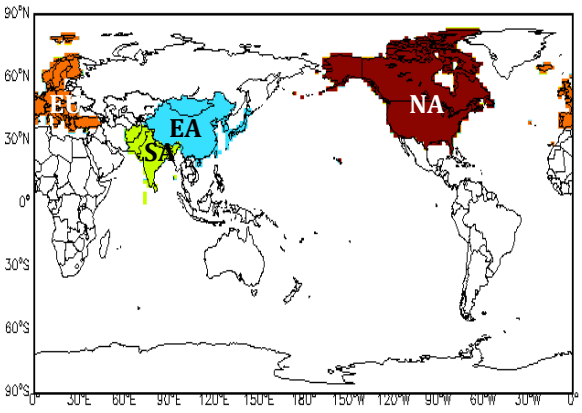

765

766 **(a)**

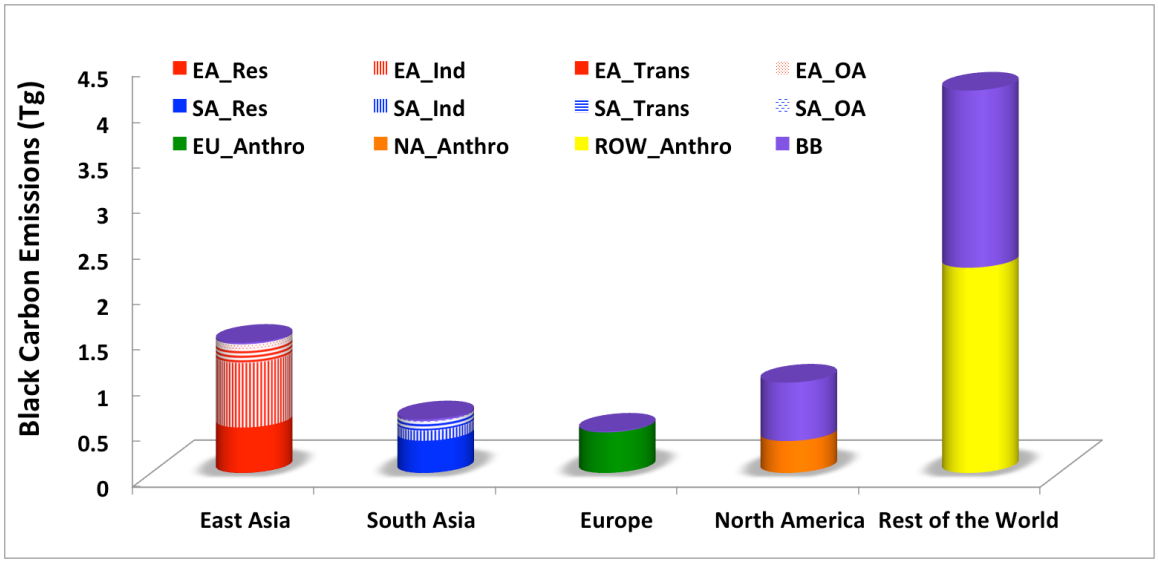

767

768 **(b)**

769 **Fig. 1 (a) Location of the four-tagged regions: East Asia (EA), South Asia (SA),**
770 **Europe (EU), and North America (NA). (b) Global annual mean land anthropogenic**
771 **and biomass burning black carbon (BC) emissions (Tg) from our tagged regions and**
772 **different sectors. Land anthropogenic (Anthro) sources include fossil fuel and biofuel**
773 **from the residential (Res), industry (Ind), land transportation (Trans), and other**
774 **(agricultural waste burning and waste management) (OA) sectors. BB (Biomass**
775 **burning) emissions include forest and grassland fires. BB emissions are not tagged**
776 **but are included in total BC emissions.**

777

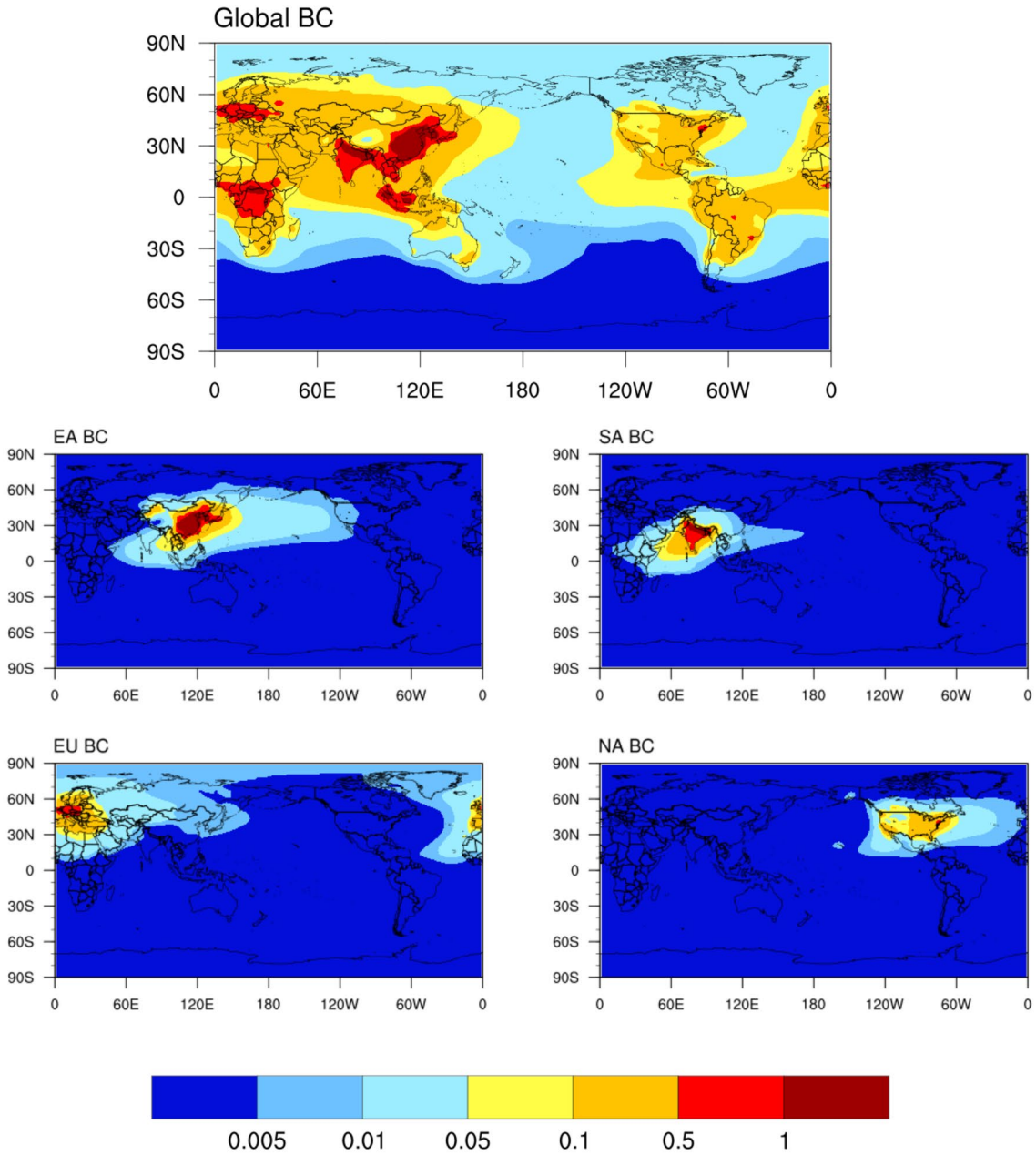

778

779 **Fig. 2 Annual average BC surface concentrations (μg/m^3) resulting from global total**

780 **BC emissions, and land anthropogenic BC emissions from each tagged region in 2000:**

781 **East Asia (EA), South Asia (SA), Europe (EU), and North America (NA).**

782

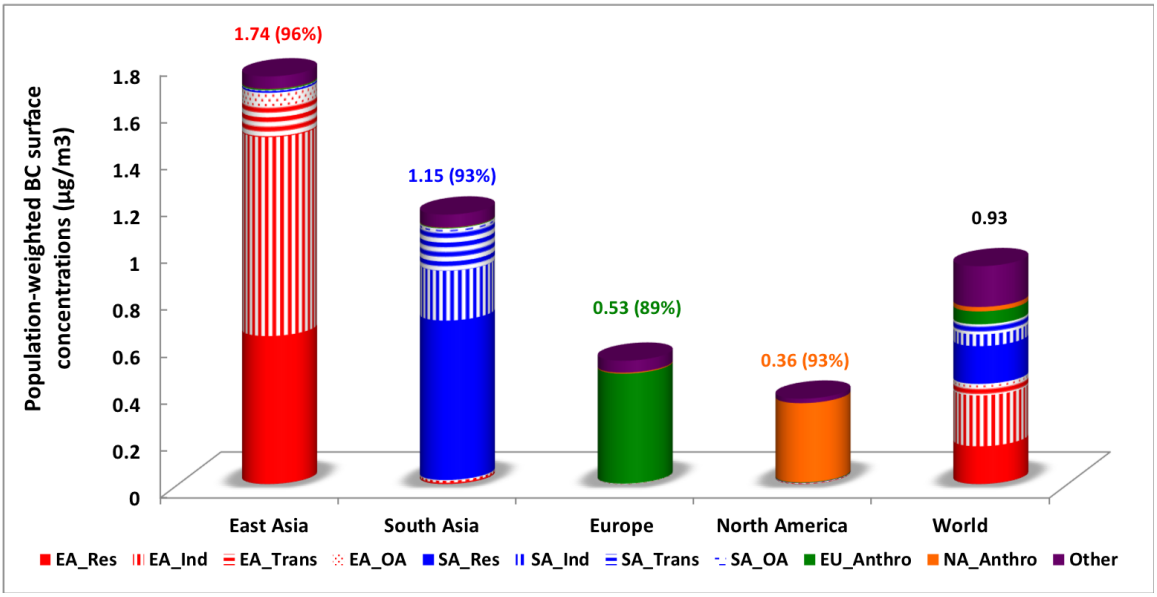

Fig. 3 Annual average population-weighted BC surface concentrations in receptor regions (µg/m^3). Percentages in parentheses represent the intra-regional contribution to annual average BC concentrations in the surface layer over each receptor region. EA, SA, EU, and NA refer to regions defined in Fig. 1a. Res, Ind, Trans, OA, and Anthro refer to the residential, industrial, and land transportation sectors plus other land anthropogenic sources (e.g., agricultural waste burning and waste management), and total land anthropogenic BC emissions, respectively. Other emissions include untagged anthropogenic emissions and biomass burning emissions.

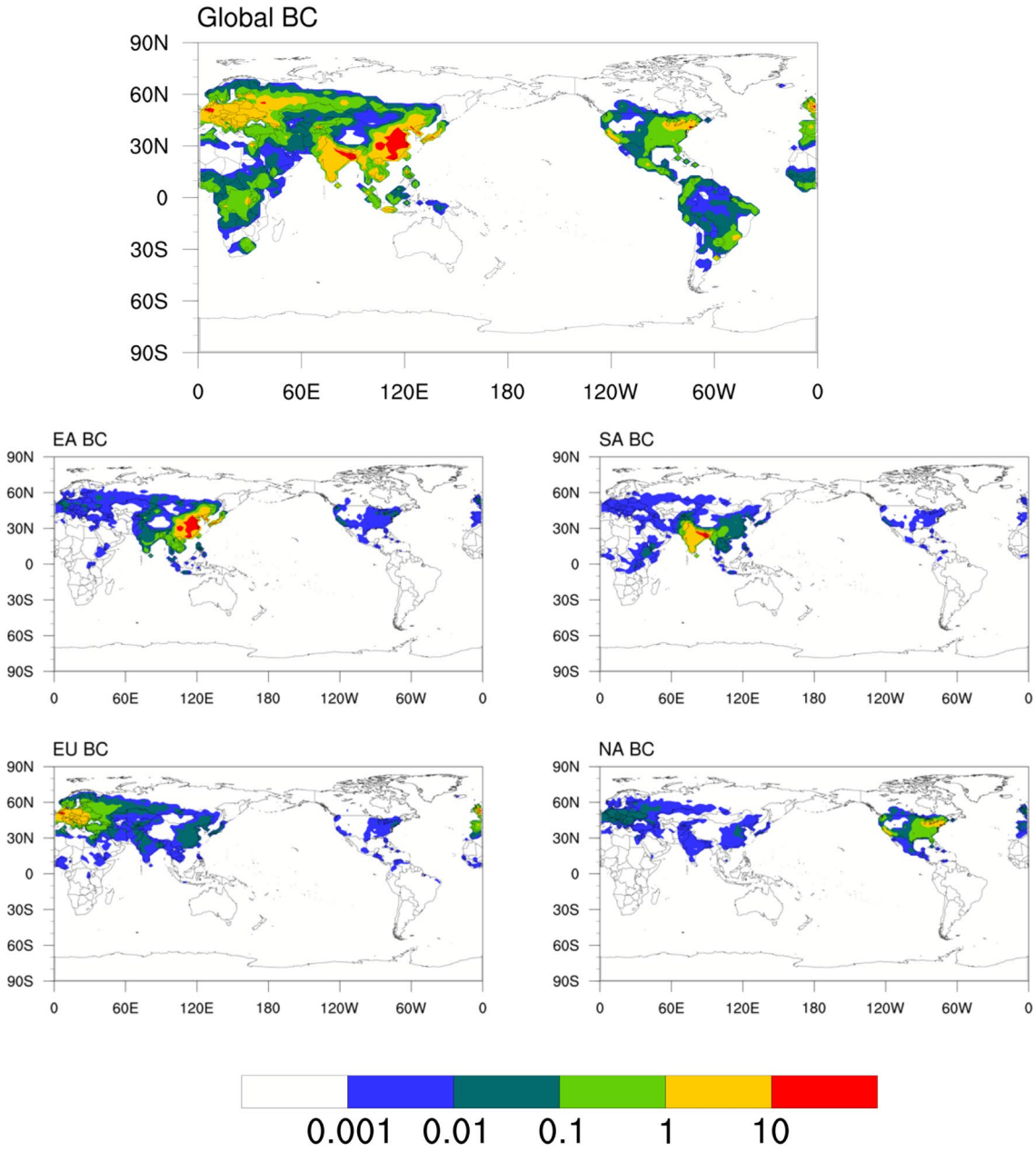

794

795 **Fig. 4 Premature mortality (deaths per 1000 km^2) associated with global total BC**

796 **emissions, and land anthropogenic BC emissions from each tagged region in 2000:**

797 **East Asia (EA), South Asia (SA), Europe (EU), and North America (NA).**

798

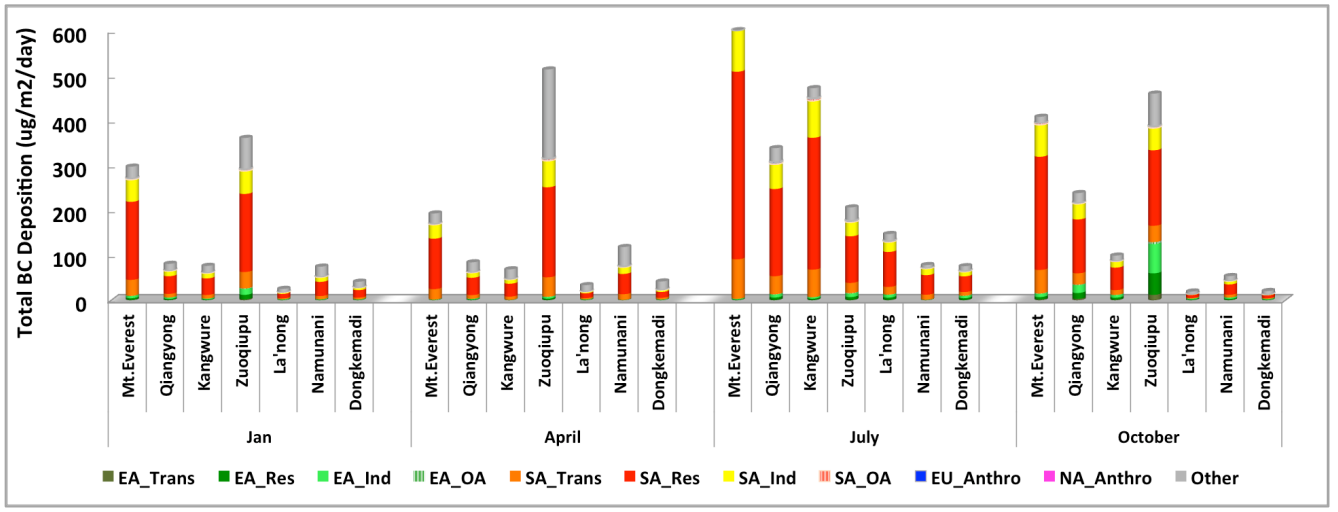

799

800 **(a)**

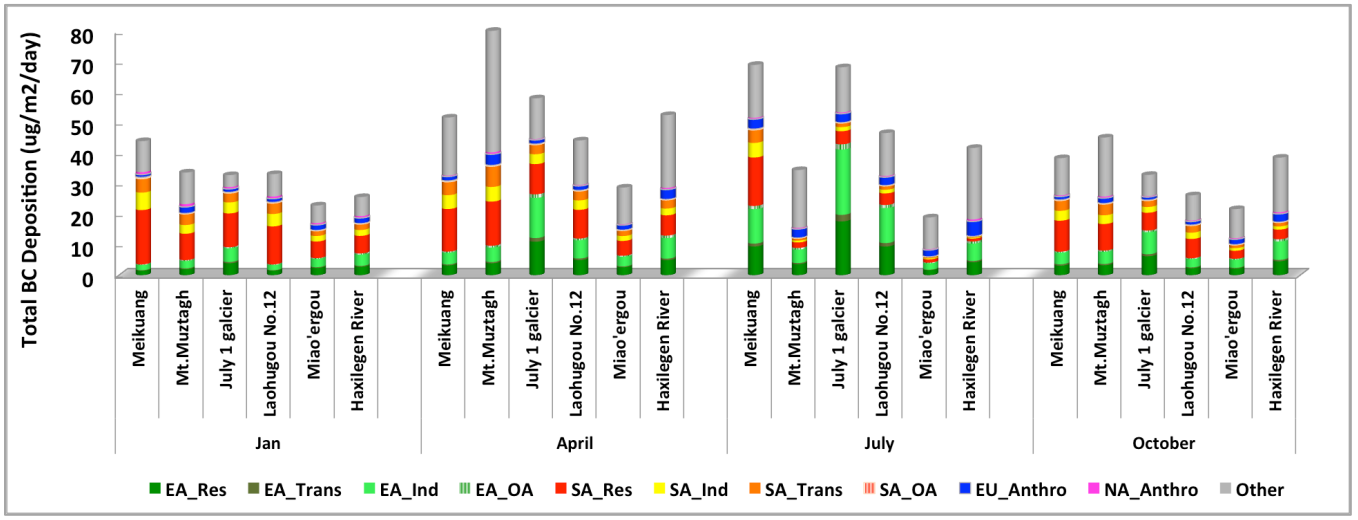

801

802 **(b)**

803

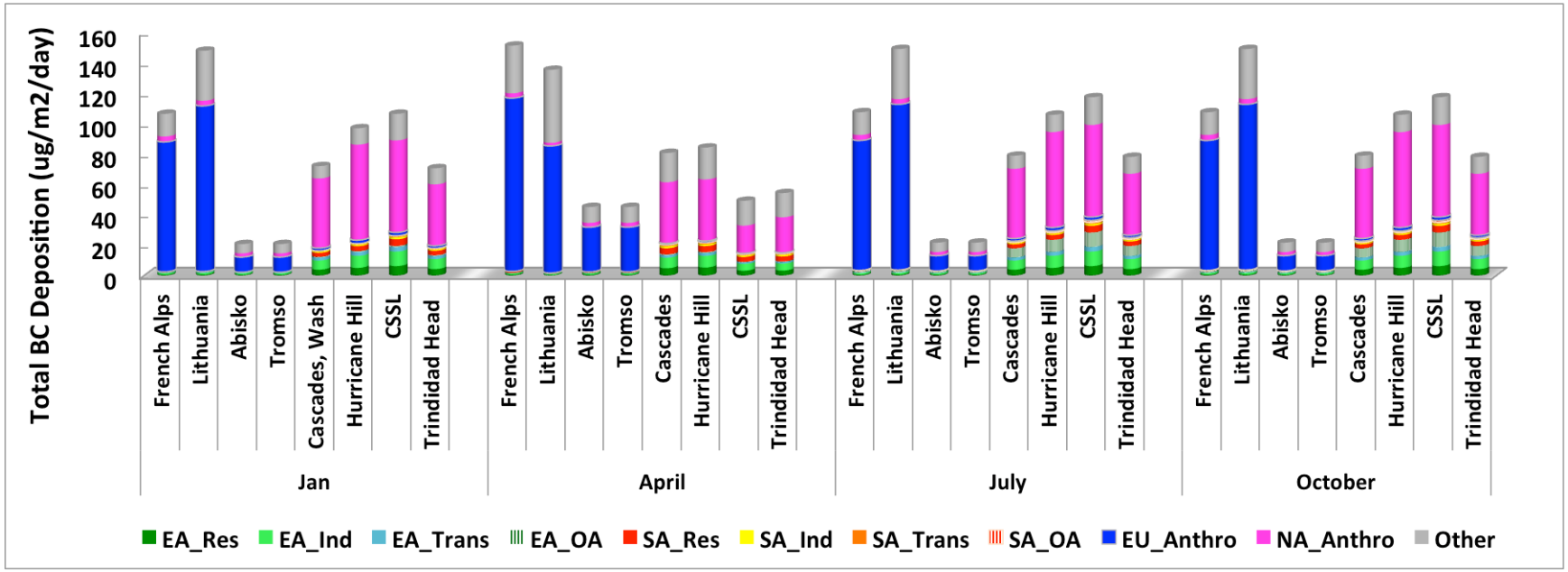

804

805 **(c)**

806

807

808

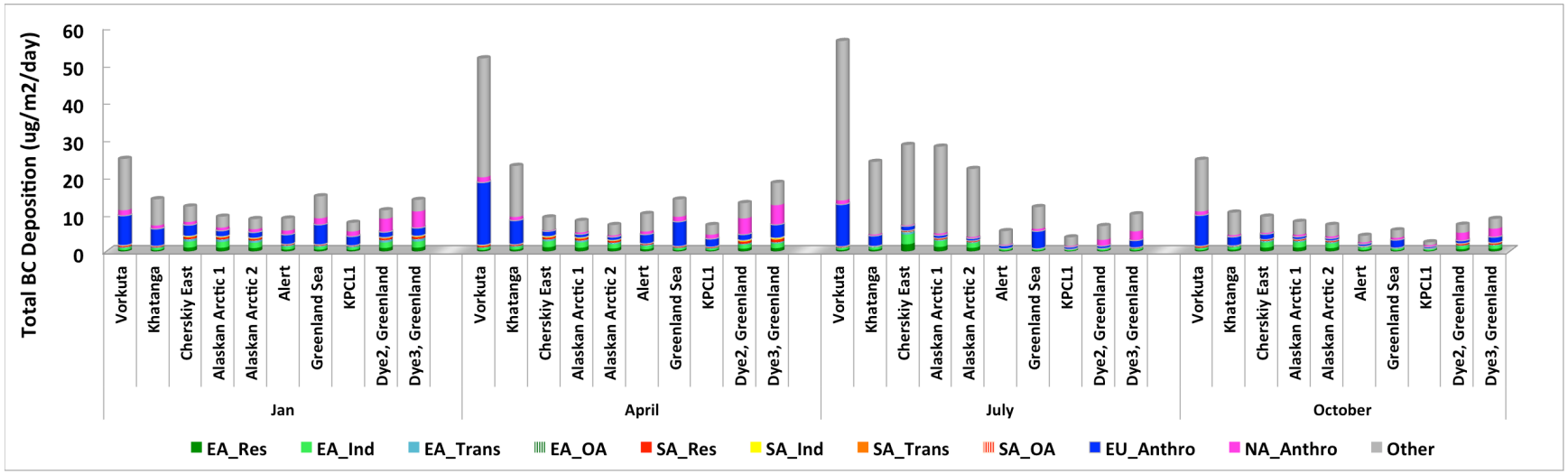

(d)

Fig. 5 Total BC deposition on glaciers (μg/m^2/day) in (a) Southern and Central Himalayas and Tibetan Plateau (HTP), (b) northern HTP, (c) Europe and North America, and (d) Arctic. Arctic glaciers located in northwestern Russia (Vorkuta), north central Russia (Khatanga), northeastern Russia (Cherskiy East), Alaska (Alaskan Arctic 1 and 2), northern Greenland (Alert, Greenland Sea, KPL1), and southern Greenland (Dye2 and Dye3). See Fig. S3 and Table S1 for glacier locations.

Table 1. Annual average premature mortality associated with BC exposure in each receptor region resulting from specific regional and sectoral sources (unit: deaths).

Sources		Receptors				
		EA	**SA**	**EU**	**NA**	**World**
Total BC		51,500 (15,600-69,400)	17,600 (8,000-27,900)	12,300 (7,300-15,500)	4,400 (2,800-4,700)	106,100 (44,900-143,400)
EA_Anthro		48,900 (95%) (14,800-65,700)	310 (2%) (96-506)	32 (0.3%) (20-42)	46 (1%) (25-65)	50,100 (47%) (15,300-67,500)
	EA_Trans	3,800 (7%) (1,500-5,000)	30 (0.2%) (9-48)	4 (0.0%) (3-5)	6 (0.1%) (3-8)	3,900 (4%) (1,500-5,300)
	EA_Res	18,100 (35%) (5,300-24,300)	120 (0.7%) (36-190)	11 (0.1%) (7-14)	16 (0.4%) (8-22)	18,500 (17%) (5,500-25,000)
	EA_Ind	24,200 (47%) (7,100-33,000)	160 (0.9%) (49-255)	16 (0.1%) (10-21)	23 (0.5%) (12-32)	24,700 (23%) (7,400-33,800)
SA_Anthro		380 (0.7%) (129-616)	16,100 (92%) (7,200-25,800)	11 (0.1%) (7-16)	14 (0.3%) (8-19)	16,800 (16%) (7,500-26,800)
	SA_Trans	65 (0.1%) (21-97)	2,600 (15%) (800-3,900)	2 (0.0%) (1-3)	2 (0.1%) (1-3)	2,700 (3%) (840-4,100)
	SA_Res	240 (0.5%) (80-390)	10,400 (59%) (4,100-16,300)	7 (0.1%) (4-10)	9 (0.2%) (5-12)	10,800 (10%) (4,300-17,000)
	SA_Ind	75 (0.1%) (25-115)	3,200 (18%) (1,000-5,000)	2 (0.0%) (1-3)	3 (0.1%) (2-4)	3,400 (3%) (1,100-5,300)
EU_Anthro		170 (0.3%) (62-215)	55 (0.3%) (19-81)	11,000 (89%) (6,500-13,800)	18 (0.4%) (12-22)	13,100 (12%) (7,700-16,000)
NA_Anthro		31 (0.1%) (11-40)	14 (0.1%) (5-21)	81 (0.7%) (50-103)	4,100 (93%) (2,600-4,300)	4,300 (4%) (2,700-4,600)

820 Total BC include emissions from all anthropogenic (land anthropogenic, aviation, and shipping) and natural sources. EA, SA, EU and
821 NA refer to tagged BC emissions from East Asia, South Asia, Europe and North America, respectively. Trans, Res and Ind refer to
822 tagged BC emissions from land transportation, residential and industrial sectors, respectively. Anthro refer to the sum of land
823 anthropogenic BC emissions in each tagged region.
824 Percentages shown in this table refer to the contributions of BC emissions from each source region and sector to total premature
825 deaths in the receptor region (i.e., EA total land anthropogenic BC emissions are responsible for 95% of total premature mortality in
826 East Asia associated with global total BC emissions).
827 Number ranges shown in this table refer to the lower and upper bound estimates in BC associated premature deaths due to
828 uncertainties in $PM_{2.5}$ relative risks.
829
830
831